Supporting Information

Transmembrane structures of amyloid precursor protein dimer predicted by replica-exchange molecular dynamics simulations

Naoyuki Miyashita,[†] John E. Straub,[‡] D. Thirumalai,[§] and Yuji Sugita*,[¶]

[†]*RIKEN Computational Science Research Program, Molecular Scale Team, 2-1 Hirosawa, Wako, Saitama 351-0198, Japan,* [‡]*Boston University, Department of Chemistry, 590 Commonwealth Ave. Boston, Massachusetts 02215-2521,* [§]*Department of Chemistry and Biochemistry and Biophysics Program, Institute for Physical Science and Technology, University of Maryland, College Park, Maryland 20742,* [¶]*RIKEN Advanced Science Institute, 2-1 Hirosawa, Wako, Saitama 351-0198, Japan*

1. Simulation Methods

In this study, we used and modified MMTSB toolset[1] with CHARMM19 EEF1.1 force field parameters.[2] The effect of solvent and membrane was introduced using effective energy function 1 (EEF1; its extension to membrane is denoted as Implicit Membrane Model 1 (IMM1)),[3] which is based on Gaussian solvent-exclusion approximation. In IMM1, (a) solvation parameters for a nonpolar phase have been introduced by using experimental data for the transfer amino acid side-chains from water to cyclohexane and (b) the distance-dependent dielectric model has been modified to account for reduced screening of electrostatic interactions in the membrane. In the preceding study[4], this model was used for predicting the dimeric structure of Glycophorin A and could reproduce the Gly-XXX-Gly interaction at the dimer interface. However, because of the approximate nature of implicit solvent model, IMM1 can't reproduce the direct interactions between lipid and polypeptide, which would be important for obtaining the potential of mean force as a function of helix-helix interaction[5]. In the current study, we focus on the dimer structures of the wild type and mutant APP fragments obtained with the implicit membrane model.

The membrane thickness was set to 30 Å. In REMD simulations, we provided 32 replicas spanning temperatures from 300 K to 500 K. Each replica was run for 22 ns (in total 704 ns). The time step was set to 2 fs and replica exchanges were performed every 2 ps. The SHAKE method was applied to bonds involved hydrogen atoms. The Nosé-Hoover algorithm was used to impose a thermostat. A cylindrical wall boundary with a radius of using 30 Å was added around two APP fragments using the MMFP module of CHARMM[2] to avoid the fragments from going far and away from each other.

The most stable conformation in our previous simulation study[6] was taken as the initial structure of an APP fragment in the REMD simulations. The two APP fragments were initially placed in the following manner:

(1) The initial inter peptide distance between the center of mass of two APP fragments was set to 20 Å.

(2) The first fragment was placed at the center of a circle with a 20 Å radius and the second fragment was placed on the circle every 360/32 degrees, preserving the same orientation.

The illustrations of peptides in all figures were prepared using VMD[7] and povray.[8]

Supporting Figures

Supporting figure 1. The amino-acid sequences of the wild type APP-C99 and a mutant, in which Gly_{29} and Gly_{33} are replaced with Leu_{29} and Leu_{33}, respectively. Gly in the transmembrane and juxtamembrane regions are shown in blue, whereas the substituted residues (Leu_{29} and Leu_{33}) are colored in red. Green residues are the terminal residues for the polypeptides used in the current simulations. β- and γ-cleavage sites are also indicated.

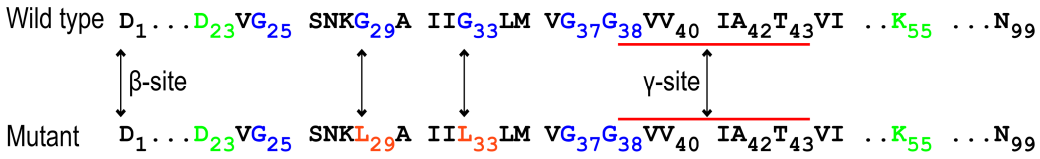

Supporting figure 2. Time-series of potential energies (a) and conformations (b) of mutant APP fragments obtained in the REMD simulations. Black dots in the time-series represent the potential energies at the highest (500 K) and the lowest (300 K) temperatures. The blue and red lines were obtained in the 30th and 10th replicas, respectively. The five conformations were obtained at the 0 ns (initial), 2.86 ns (1), 7.60 ns (2), 13.90 ns (3), and 19.88 ns (4) in the 10th replica's trajectory.

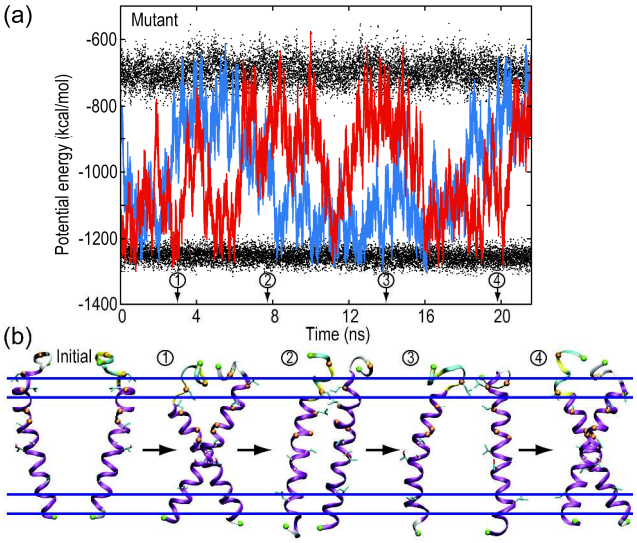

Supporting figure 3. The averaged tilt angle of APP fragments along the z-axis (bilayer normal). The α-helix was defined using backbone atoms from Gly_{38} to Lys_{55}. The red and blue boxes represent the averaged tilt angle of two fragments in the wild type and the mutant, respectively.

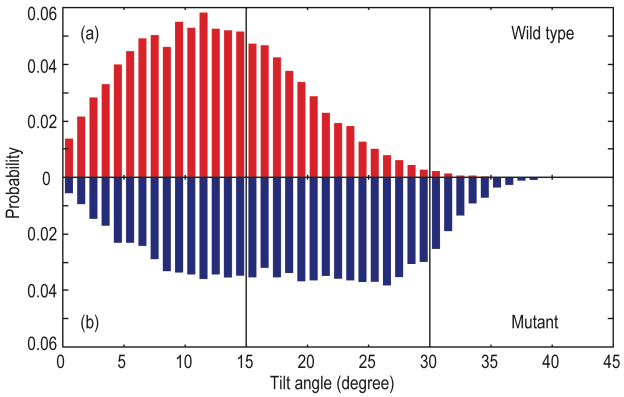

Supporting figure 4. Projection of the simulation trajectories at 300 K to the principal component axes for wild type (a) and the mutant (b) proteins. The contributions of the first three principal components are 22.15%, 12.16%, and 9.55%. The first and third principal components (PC1 and PC3) were taken, because these axes could clearly classify the mutant APP dimer conformations. PM1 (65.4 %), and PM2 (28.5 %) are the two most representative clusters observed in the mutant. In contrast, the WT dimer conformations crowded on the center and were not well classified in the analysis. PW1 indicates the most populated structure in the WT.

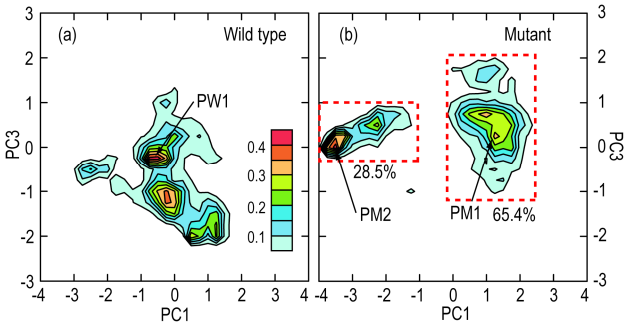

Supporting figure 5. Two-dimensional distribution of the C_α distance between Gly_{33}-Gly_{33} and the minimum C_α distance between Gly_{33}-Gly_{38} of the wild type fragments. The most populated structure is indicated as PW1 (31.1%).

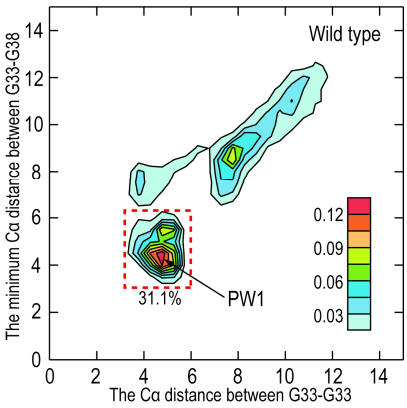

Supporting figure 6. Probability distributions of the C_α distances between two APP fragments. (a) the wild-type Gly_{33}-Gly_{33} and the mutant Leu_{33}-Leu_{33}, (b) Gly_{38}-Gly_{38} for wild type and the mutant, and (c) Gly_{33}-Gly_{38} for wild type. The probabilities for the nearest and furthest pairs were counted separately.

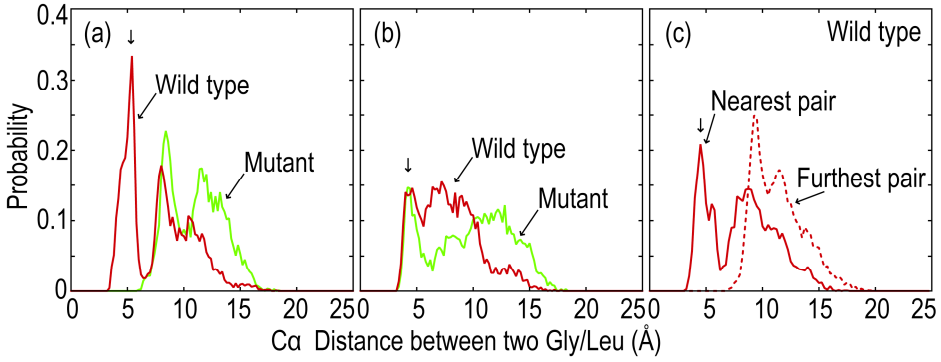

2. References

1. Feig, M.; Karanicolas, J.; Brooks, C. L. *J. Mol. Graphics and Modeling* **2004**, *22*, 377-395.
2. MacKerell, A. D. Jr.; Bashford, D.; Bellott. M.; Dunbrack, R. L.; Evanseck, J. D.; Field, M. J.; Fischer, S.; Gao, J.; Guo, H.; Ha, S.; Joseph-McCarthy, D.; Kuchnir, L.; Kuczera, K.; Lau, F. T. K.; Mattos, C.; Michnick, S.; Ngo, T.; Ngyuen, D. T.; Prodhom, B.; Reiher, W. E. III; Roux, B.; Schelenkrich, M.; Smith, J. C.; Stote, R.; Straub, J. E.; Watanabe, M.; Wiókiewicz-Kuczera, J.; Yin, D.; Karplus, M. *J. Phys. Chem. B* **1998**, *102*, 3586-3616.
3. (a) Lazaridis, T.; Karplus, M. *Proteins* **1999**, *35*, 133-152. (b) Lazaridis, T. *Proteins* **2003**, *52*, 176-192.
4. Mottamal, M.; Zhang, J.; Lazaridis, T. *Proteins* **2006**, *62*, 996-1009.
5. Lee, J.; Im, W. *J. Am. Chem. Soc.* **2008**, *130*, 6456-6462.
6. Miyashita, N.; Straub, J. E.; Thirumalai, D. *to be published.*
7. Humphrey, W.; Dalke, A.; Schulten, K. *J. Mol. Graphics* **1996**, *14*, 33-38.
8. http://www.povray.org